First publ. in: Journal of Molecular Biology 391 (2009), 2, pp. 498-507

Complete Ion-Coordination Structure in the Rotor Ring of Na^+-Dependent F-ATP Synthases

Thomas Meier[1,2]*, Alexander Krah[3]†, Peter J. Bond[3]†, Denys Pogoryelov[1], Kay Diederichs[4] and José D. Faraldo-Gómez[2,3]*

[1]*Department of Structural Biology, Max Planck Institute of Biophysics, Max von Laue Strasse 3, 60438 Frankfurt am Main, Germany*

[2]*Cluster of Excellence Macromolecular Complexes, Max Planck Institute of Biophysics, Max von Laue Strasse 3, 60438 Frankfurt am Main, Germany*

[3]*Theoretical Molecular Biophysics Group, Max Planck Institute of Biophysics, Max von Laue Strasse 3, 60438 Frankfurt am Main, Germany*

[4]*Department of Biology, University of Konstanz, 78457 Konstanz, Germany*

Received 4 May 2009; received in revised form 28 May 2009; accepted 29 May 2009
Available online 3 June 2009

Edited by J. Bowie

The membrane-embedded rotors of Na^+-dependent F-ATP synthases comprise 11 c-subunits that form a ring, with 11 Na^+ binding sites in between adjacent subunits. Following an updated crystallographic analysis of the c-ring from *Ilyobacter tartaricus*, we report the complete ion-coordination structure of the Na^+ sites. In addition to the four residues previously identified, there exists a fifth ligand, namely, a buried structural water molecule. This water is itself coordinated by Thr67, which, sequence analysis reveals, is the only residue involved in binding that distinguishes Na^+ synthases from H^+-ATP synthases known to date. Molecular dynamics simulations and free-energy calculations of the c-ring in a lipid membrane lend clear support to the notion that this fifth ligand is a water molecule, and illustrate its influence on the selectivity of the binding sites. Given the evolutionary ascendancy of sodium over proton bioenergetics, this structure uncovers an ancient strategy for selective ion coupling in ATP synthases.

Keywords: F_1F_o-ATP synthase rotor; c-ring structure; ion coordination and selectivity; sodium-motive force; *Ilyobacter tartaricus*

Introduction

Adenosine triphosphate (ATP) is the universal energy currency in all living cells, sustaining many and diverse biochemical reactions and processes. F-type ATP synthases are the main producers of ATP; these large protein complexes are found in the membranes of mitochondria, chloroplasts, and bacteria, and power their enzymatic activity with the dissipation of electrochemical gradients across these membranes. Remarkably, these enzymes can also operate in reverse and act as transmembrane ion pumps, thereby using the energy derived from the hydrolysis of ATP to establish a concentration gradient.

Structurally, F-type ATP synthases comprise two distinct subcomplexes referred to as F_1 and F_o. While the synthesis or hydrolysis of ATP takes place in the water-soluble F_1 region,[1,2] the membrane-embedded F_o complex acts as a rotor that is coupled to the translocation of protons or sodium ions across the membrane. The bacterial F_o complex

*Corresponding authors. E-mail addresses: thomas.meier@biophys.mpg.de; jose.faraldo@biophys.mpg.de.

† A.K. and P.J.B. contributed equally to this work.

Abbreviations used: PDB, Protein Data Bank; MD, molecular dynamics; POPC, 1-palmitoyl-2-oleoyl-*sn*-glycero-3-phosphocholine; *smf*, sodium-motive force; *pmf*, proton-motive force.

consists of three membrane-anchored subunits with a stoichiometry of ab_2c_{10-15}. The c-subunits form a ring-like structure, with subunits a and b_2 assembled laterally. Both F_1 and F_o complexes can be seen as individual molecular motors connected by a central bearing (γ-subunit) that acts as a transducer of mechanical energy between them (for reviews, see Capaldi and Aggeler,[3] Yoshida *et al.*,[4] and Nakamoto *et al.*[5]).

The mechanism that couples the transmembrane movement of protons or sodium ions to the rotation of the c-ring is not fully understood. Biochemical studies, though, have clearly shown that cations (Na^+) do bind to the c-ring.[6,7] The crystal structure of the rotor from the *Ilyobacter tartaricus* Na^+-dependent ATP synthase provided atomic detail to this notion.[8] In this structure, each c-subunit consists of two α-helices connected by a short cytoplasmic loop, with the N-terminus and C-terminus located in the periplasm. The ring comprises 11 subunits, which form a symmetric hourglass-shaped assembly. In between each pair of adjacent subunits, a Na^+ binding site can be clearly identified. The coordination shell for this ion is composed of the side-chain oxygen atoms of Gln32 and Glu65 of one subunit and, from the adjacent subunit, the hydroxyl oxygen of Ser66 and the backbone carbonyl oxygen of Val63. Notably, Glu65 acts not only as one of the four Na^+-binding ligands but also as an acceptor of three hydrogen bonds from the amine and hydroxyl groups of Gln32, Ser66, and Tyr70, respectively. This arrangement, present in all 11 binding sites, appears to provide a stable locked conformation of the site, where the interaction of Na^+ with protein ligands, especially Glu65, compensates for the energetic cost of its desolvation and transfer into the membrane. It also follows from this observation that ion exchange within the a/c interface during enzyme activity is likely to be accompanied by conformational changes in the binding site.[8] In particular, a reversible interaction with a positively charged arginine in the stator subunit a[9,10] is believed to be crucial for the sequential loading and unloading of the binding site as the c-ring rotates.[11]

An almost identical coordination structure was found in the crystal structure of the K-ring of the V-type ATPase from *Enterococcus hirae*.[12] In this enzyme, the K-ring also acts as a rotary subunit powered by ATP hydrolysis, thereby pumping Na^+ across the membrane. Intriguingly, however, the K-ring was found to contain an additional fifth coordinating site, namely, the side-chain carbonyl of Gln65. At physiological pH, both the *I. tartaricus* ATP synthase[13] and the *E. hirae* ATPase preferentially select Na^+ during enzyme operation.[14] This means that the binding sites of both c-ring and K-ring must be selective against all other cations under such conditions. Indeed, available data indicate that they are and to a similar degree.[6,7,13,15–17] Considering how slight are the differences between these cations (e.g., Na^+ and K^+ differ by less than 0.4 Å in radius), it seems odd that the lack of one coordination site in the *I. tartaricus* c-ring would result in no functional difference with the K-ring from *E. hirae*. Moreover, a recent survey of Na^+ binding sites in the Protein Data Bank (PDB; selective and nonselective) shows that the most prominent coordination number is 5, consistent with the observation for the K-ring, while a coordination number of 4 is about twofold less frequent.[18]

Prompted by these considerations, we set out to reexamine the crystallographic data for the *I. tartaricus* c-ring, and we report here the existence of additional electron density within the coordination shell of all Na^+ in the structure. This density appears to correspond to a water molecule buried between Na^+ and the inner α-helix. To examine this hypothesis further, we employ molecular dynamics (MD) simulations of the complete c-ring embedded in a lipid membrane and calculations of the binding affinity of this structural water. The results from these calculations are clearly consistent with the notion that a buried water molecule is the fifth coordinating ligand for Na^+. Further computations are presented to illustrate the importance of this fifth site for the selective ion-binding properties of the rotor in ATP synthases.

Results

Crystallographic analysis of the Na^+ binding site

During the process of solving the original structure of the c-ring from *I. tartaricus*,[8] 513 electron density peaks were assigned to crystalline water molecules (PDB ID code 1yce). A total of 44 bound Na^+ ions, 11 in each of the four rings in the asymmetric unit, could also be clearly identified through valence screening.[19] In some regions, however, the electron density derived from the diffraction data could not be interpreted with confidence. Intriguingly, several of these unassigned peaks were observed in close proximity to the bound Na^+, but this density was apparent only in a fraction of the sites (Fig. S1). Given this and the resolution limit of the data, at 2.4 Å, the interpretation of this density was uncertain. Thus, at the time, it was concluded that the coordination shell of Na^+ was limited to four oxygen ligands from the protein, as explained previously.

In view of the coordination structure observed in the V-ATPase K-ring from *E. hirae*[12] and bearing in mind recent statistical surveys of metal coordination in proteins,[18,20] this conclusion deserves further examination. Specifically, it appears plausible that the weak electron density that was detected in the vicinity of the bound Na^+ in the c-ring corresponds to an additional coordination site, presumably in the form of a water molecule. To evaluate this hypothesis, we decided to recalculate the structure from the original X-ray diffraction data, using the latest available versions of crystallography software for data reduction and refinement. The final model has

Table 1. Summary of data collection and refinement statistics

	This work
Data processing	
Wavelength (Å)	0.9756
Space group	$P2_1$
Unit cell parameters *a*, *b*, *c* (Å)	146.7, 139.3, 151.9
Unit cell parameters α, γ, β (°)	90, 90, 118.4
Solvent content (%)	66.1
Resolution (Å)	40.0–2.35 [2.45–2.35][a]
Number of observed reflections	2,424,596 [178,827]
Number of unique reflections	220,545 [23,835]
Completeness (%)	98.7 [91.2]
R_{meas} (%) (2)	18.2 [117.1]
$R_{mrgd}-F$ (%) (2)	18.3 [117.6]
I/σ_I	8.83 [1.77]
Refinement statistics	
Resolution (Å)	40–2.35 [2.38–2.35][a]
R-factor (%)	22.0 [34.0][a]
R_{free} (%)R_{free}	24.5 [38.3][a]
Number of residues	3916
Number of solvent waters	423
Number of ions	44
Number of fatty acid chains	44
RMSD of bond length (Å)	0.012
RMSD of bond angles (°)	0.704
Average RMSD of main-chain [side side-chain] atom positions between the old model (PDB ID code 1yce) and the new model (PDB ID code 2wgm) (Å)	0.39 [0.48]

[a] Numbers in brackets correspond to the highest-resolution shell.

a resolution of 2.35 Å; the resulting statistics from this updated analysis are summarized in Table 1.

Figure 1 shows the Na^+ binding site in this improved structure of the c_{11}-ring from *I. tartaricus* ATP synthase. With regard to the protein ligands, the coordination structure of the cation is essentially identical with that previously reported,[8] and the conformations of all side chains in and near the site are unequivocal. Importantly, the additional density in the vicinity of the ion can now be unambiguously discerned in all binding sites in the unit cell, as shown for one complete c-ring (Fig. 1b and c). Based on geometric considerations (Table 2), this density indeed appears to correspond to a buried water molecule, which not only coordinates Na^+ and therefore completes the 5-coordination shell but also is an integral part of the structure of the site as it forms hydrogen bonds with the carbonyl oxygen of Ala64 and with the hydroxyl oxygen of Thr67.

MD and free-energy calculations

To complement the crystallographic analysis, we provide three pieces of evidence derived from atomically detailed MD simulations of the full c-ring embedded in a 1-palmitoyl-2-oleoyl-*sn*-glycero-3-phosphocholine (POPC) membrane (~100,000 atoms). The first of these arguments is the binding affinity of the water molecule that, as we proposed, coordinates Na^+. To calculate this quantity, we follow an approach that has been previously used for the bacteriorhodopsin proton channel.[21] That is, we computed the free-energy cost of extracting a water molecule from the bulk solution and the free energy gained by inserting it into the site identified in the electron density map of the protein crystal. These values are $-\Delta G_{bulk}=6.5\pm0.1$ kcal/mol and $\Delta G_{site}=-12.6\pm0.2$ kcal/mol, respectively. From these values, we can now derive the standard binding free energy ΔG_b° using the expression:

$$\Delta G_b^\circ = \Delta G_{site} - \Delta G_{bulk} - k_B T \log C^\circ V_{site}$$

where k_B is the Boltzmann constant and T is the temperature (298 K). The last contribution in the equation above reflects loss of translational entropy upon binding, which is defined in terms of the accessible volume for the ligand at the site V_{site} relative to the standard state volume $1/C^\circ = 1661$ Å^3.[22,23] From the extent of the motions of the water molecule at the binding site during our simulations, we estimate that $V_{site}=4.2$ Å^3 (i.e., this entropic penalty is 3.6 kcal/mol). The resulting binding free energy is therefore -2.5 ± 0.2 kcal/mol, that is to say, $K_d=\exp(\Delta G_b^\circ/k_BT)\approx 15$ mM. This dissociation constant can be related to the probability of occupancy:

$$P_o = [1 + K_d/a_w C]^{-1}$$

where $C=55.5$ M is the concentration of water, and a_w is water activity. Under ideal conditions, $a_w=1$ and, therefore, $P_o\sim0.9997$. In the crystallization cryobuffer,[8] a_w is only slightly reduced to ~0.95,[24,25] and so P_o is unchanged (within four decimal digits). We thus conclude that, at least from a thermodynamic standpoint, the presence of this water molecule in the binding site is unequivocal.

The second line of evidence derives from conventional MD simulations of the complete sodium-loaded c-ring in the presence and in the absence of the coordinating water molecule. These simulations reveal that, in the absence of the key water molecule, the side chain of Thr67 would alternatively adopt two rotameric states (Fig. 2). In one of these states, referred to as rotamer A, its hydroxyl group hydrogen bonds to the backbone carbonyl of Gly25 in the adjacent c-subunit; this is the rotamer observed in the crystal structure. In the other state, or rotamer B, the hydroxyl group directly coordinates with Na^+, which becomes slightly displaced. As illustrated in Fig. 2a, the exchange between these two states occurs on the nanosecond timescale. Within the duration of the simulation (15 ns), it was observed in all 11 binding sites. Altogether, in the hypothetical situation where Na^+ lacks a fifth coordination site, rotamer B would be about three-fold more probable than rotamer A (Fig. 2b) and would effectively become the fifth site. Although this finding is intriguing, analysis of the electron density maps of the isolated c-ring of *I. tartaricus* is not consistent with the notion that Thr67 adopts rotamer B. Given that the interconversion rate between these rotamers is likely to be faster (nanoseconds) than the flashcooling of the protein

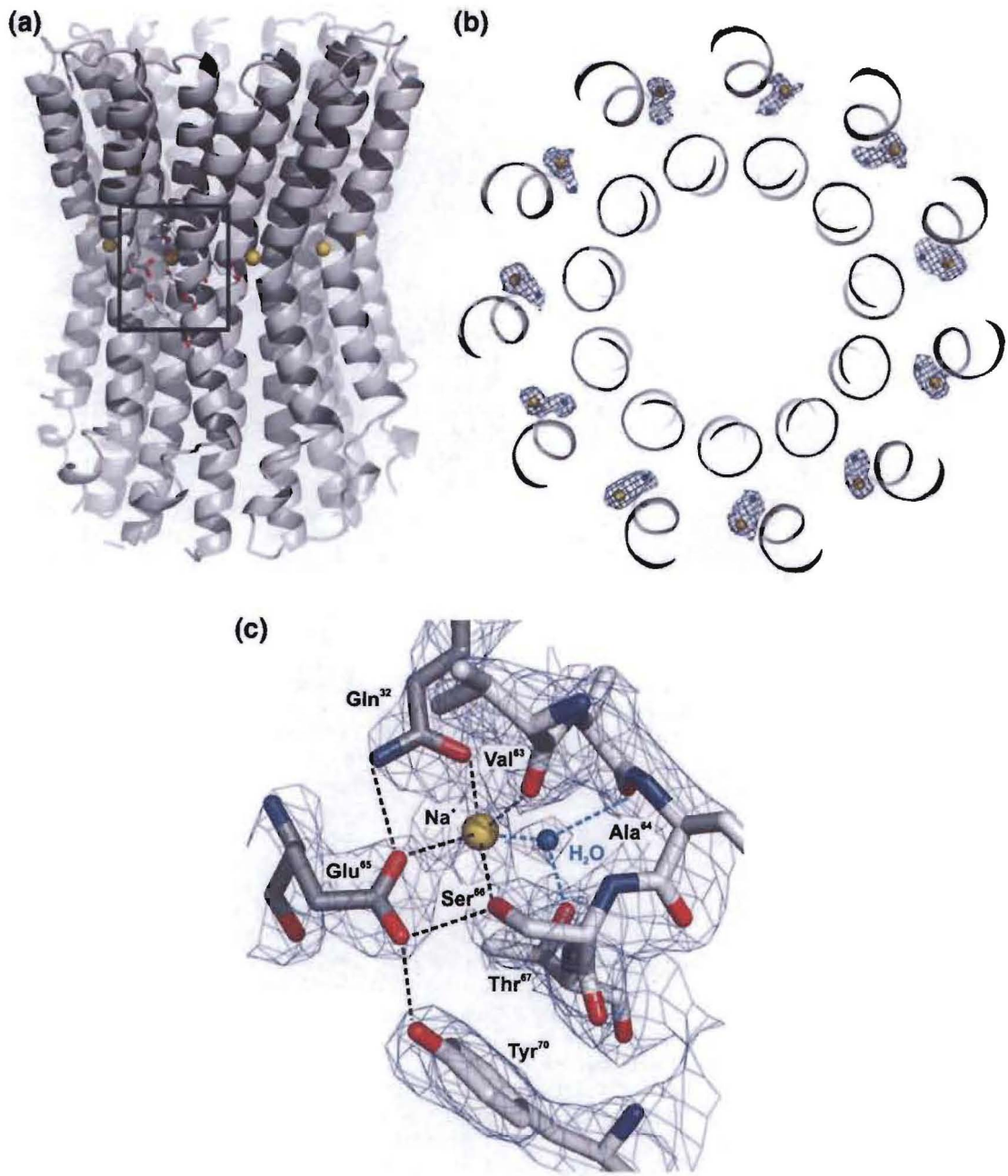

Fig. 1. The Na^+ binding site in the c_{11}-ring from *I. tartaricus* ATP synthase. (a) The ring is composed of 11 c-subunits, each comprising two transmembrane helices shown as gray ribbons. The binding sites for Na^+ (yellow spheres) are located in between adjacent subunits. (b) Nonsymmetrized electron density peaks ($2F_{obs}-F_{calc}$ map at 1.8σ) corresponding to buried structural water molecules (blue spheres) that coordinate Na^+ (yellow spheres). The view is of a slice of density parallel with the plane of the membrane. (c) Close-up and electron density map of the Na^+ binding site ($2F_{obs}-F_{calc}$ map at 1.8σ) from the same viewpoint as the rectangle in (a). The amino acids involved in ion coordination are depicted in stick representation. Thr67 and Ala64 are also indicated (see Results). Ion–protein contacts and the network of hydrogen bonds in the site are indicated with broken lines.

crystals in liquid nitrogen, one would certainly expect to detect electron density for rotamer B if such state were to exist.

By contrast, the simulation of the c-ring that includes the water molecule in the cation site reveals absolutely no exchange between rotamers in Thr67 for any of the binding sites, consistent with the electron density. Rather, the hydroxyl oxygen of Thr67, along with the carbonyl of Ala64, provides robust hydrogen-bonding interactions that help to orient the molecular dipole of the water in a way that is optimal for the coordination of Na^+ and appears to help sustain the overall structure of the coordination shell.

Table 2. Interatomic distances at the Na^+ binding site of the *I. tartaricus* c-ring

From	To	Distance (Å)[a]	RMSD
Na^+	Gln32 $O^{\varepsilon 1}$	2.39	0.09
Na^+	Val63 O	2.38	0.09
Na^+	Glu65 $O^{\varepsilon 2}$	2.48	0.10
Na^+	Ser66 O^{γ}	2.26	0.10
Na^+	HOH	2.37	0.14
HOH	Thr67 $O^{\gamma 1}$	2.75	0.11
HOH	Ala64 O	2.79	0.11
Glu65 $O^{\varepsilon 2}$	Gln32 $N^{\varepsilon 2}$	2.83	0.02
Glu65 $O^{\varepsilon 1}$	Tyr70 OH	2.77	0.04
Gly25 O	Thr67 $O^{\gamma 1}$	2.67	0.03
Ser66 O^{γ}	Glu65 $O^{\varepsilon 1}$	2.60	0.04

[a] The values shown are averages, with the corresponding RMSD taken over the 11 sites present in each ring and the four rings found in the asymmetric unit cell. Structural refinement was carried out without noncrystallographic symmetry restraints on Na^+ and HOH positions. The distances between Na^+ and surrounding atoms were also not restrained (default van der Waals repulsion forces were switched off) and were therefore unbiased.

Our third and final argument derives from free-energy calculations of the cation selectivity of the binding site. For these calculations, we adopt an approach analogous to that in previous studies of selective ion channels and ion-coupled membrane transporters.[18,26,27] That is, we construct a thermodynamic cycle that allows us to express the free energy of selectivity between two cations, $\Delta\Delta G_{sel}$ ($C_1^+ \rightarrow C_2^+$), in terms of the energy cost or gain upon a nonphysical transformation between them, both at the binding site and in the bulk:

$$\Delta\Delta G_{sel}(C_1^+ \rightarrow C_2^+) = \Delta G_{site}(C_1^+ \rightarrow C_2^+) - \Delta G_{bulk}(C_1^+ \rightarrow C_2^+)$$

Further details, including a comparison of computed and measured selectivity free energies for the K-ring of the V-ATPase from *E. hirae*, can be found in Materials and Methods and Supplementary Data.[17] Using the same approach and force-field parameters for the *I. tartaricus* c-ring, we assess whether the water molecule in question is required to yield the correct selectivity. Based on the results shown in Table 3, we conclude that this is indeed the case. By contrast, the selectivity values computed in the absence of the coordinating water cannot be reconciled with experimental observations. Specifically, competitive binding assays based on inhibition of ATPase activity through DCCD labeling of Glu65[7] indicate that the selectivity against K^+ should be greater than +3.7 kcal/mol (or $K_i/K_d > 500$). An analogous threshold can be derived for the V-ATPase K-ring, which shows no K^+ binding even at a 1000-fold concentration excess over Na^+ (i.e., $\Delta\Delta G_{sel} > 4.1$ kcal/mol).[17] The computed value of 2.5 kcal/mol in the absence of the water molecule is well below this lower-bound estimate. Similarly, the selectivity against Li^+ in the absence of the coordinating water is significantly reduced relative to the experimental estimate of 1.4 kcal/mol (i.e., 10-fold smaller affinity than Na^+).[7,15] Taken altogether, we conclude not only that there is a fifth coordination site for Na^+ in the form of a water molecule but also that this additional ligand is crucial for the selectivity properties of the c-subunit.

Discussion

In this study, we have complemented crystallographic data with *in silico* methods to unequivocally demonstrate that a buried water molecule provides a fifth interaction site for Na^+ in the rotor subunit of the F-type ATP synthase from *I. tartaricus*. This finding allows us to reconcile the ion selectivity properties of this ring with the chemical structure of the binding site (Fig. 3). The interaction of this key water molecule with Thr67 also provides new insights into the complex question of what distinct chemical and structural features determine Na^+ *versus* H^+ coupling in ATP synthases—that is to say, into the evolutionary transition between cellular bioenergetics driven by the sodium-motive force (*smf*) and the proton-motive force (*pmf*).[28]

To date, only four ATP synthases have been shown biochemically to be coupled to Na^+ transport, all of which are found in anaerobic bacteria. The first ATP synthase of this type was discovered in the bacterium *Propionigenium modestum*[29] and, subsequently, also in *Acetobacterium woodii*,[30] *I. tartaricus*,[13] and *Clostridium paradoxum*.[31] Nonetheless, the *smf* has been recently postulated as the ancestral type of membrane energy metabolism, as it would be advantageous over the *pmf* in high pH environments or at high temperatures.[32,33] Therefore, the structure of the Na^+-binding c-ring presented here provides us with an insight into a strategy for ATP synthesis that was already present in the early history of life, rather than simply an unusual adaptation of a minor fraction of exotic bacterial strains.

In Fig. 4, we have aligned the amino acid sequences of the c-subunits in all known Na^+-dependent species alongside those representative of their H^+-coupled homologues (and of the K-ring from *E. hirae*). From this comparison, it is clear that there exists a sequence signature in the binding sites of the Na^+-dependent c-subunits, namely, Gln32, Glu65, Ser/Thr66, Thr67, and Tyr70 (*I. tartaricus* numbering). This observation is consistent with the structure of the *I. tartaricus* c-ring[8] and also with mutagenesis data for the closely related *P. modestum*.[34] However, it is also clear that among these amino acids, only Thr67 is distinctive of the sodium-dependent subfamily. In all of the known proton-coupled ATP synthases such as those from spinach chloroplasts[35] or from the cyanobacterium *Synchocystis* sp. strain PCC 6803,[36] Thr67 is replaced by a hydrophobic bulkier amino acid. This substitution very likely precludes the presence of a water molecule in the binding site and would therefore limit the number of possible coordinating ligands, which may contribute to their specificity. It will be therefore very interesting to elucidate the unknown ion-binding properties of putative ATP synthases

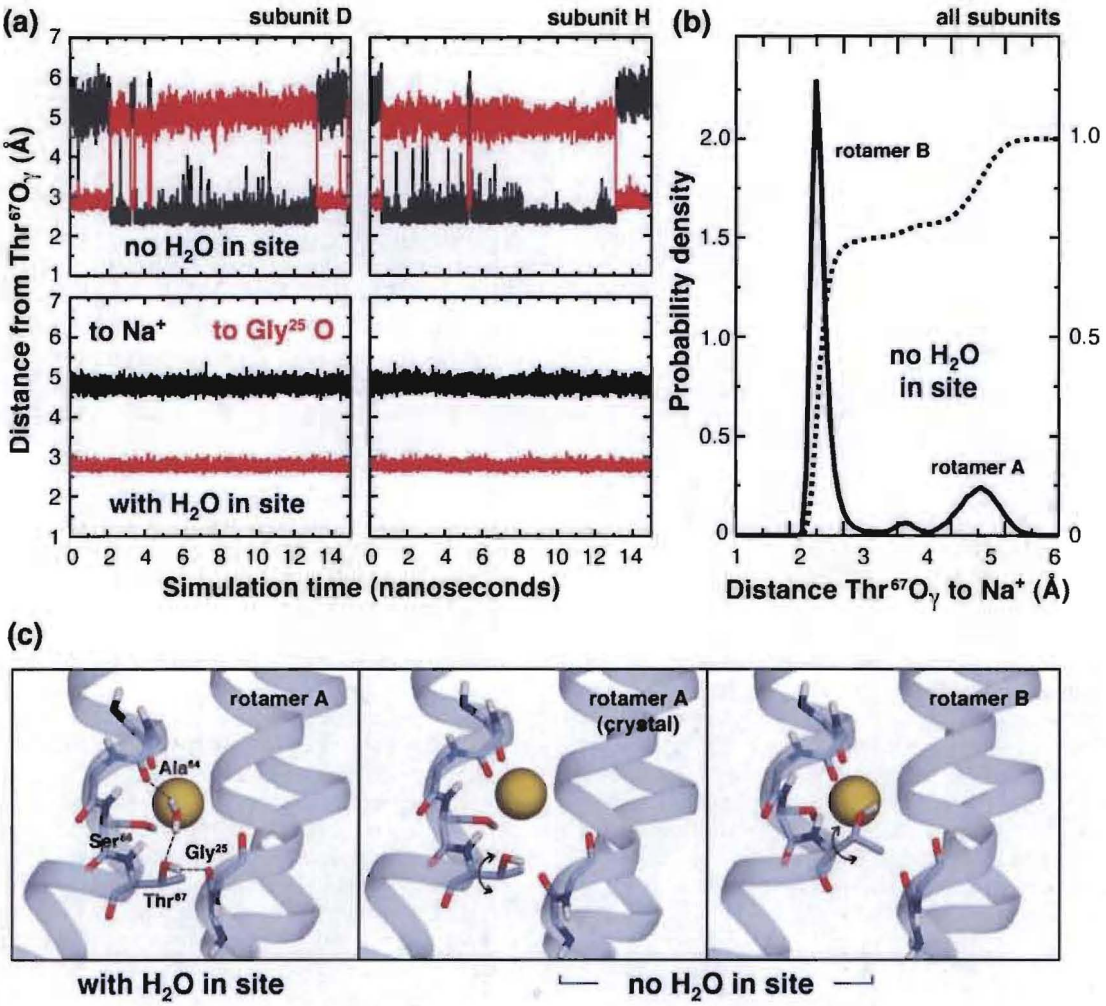

Fig. 2. Influence of the Na^+-coordinating water molecule on the dynamics of Thr67. (a) The distance between the hydroxyl O^γ atom of Thr67 and either the carbonyl O atom of Gly25 (red) or Na^+ (black) is plotted for two representative subunits in the ring. The data derive from independent simulations in the presence (bottom) and in the absence (top) of the water molecule. (b) Relative probabilities of rotamers A and B, in the absence of the coordinating water molecule, derived from the time series depicted in (a), combining all 11 binding sites. The broken curve represents cumulative probability. (c) Left to right: Randomly selected simulation snapshots of the binding site for Na^+ (yellow) in the presence and in its absence of the coordinating water molecule; in the latter case, rotamers A and B of Thr67 are shown. For clarity, only a subset of the side chains comprising the binding site is depicted.

that also include a threonine residue at this position, such as the human pathogenic family of *Mycoplasma* strains (Fig. 4). The bacteria having this threonine in their c-subunit sequences belong to different phyla (Fusobacteria, Firmicutes, Tenericutes, and Thermotogae) whose only common characteristic is that they grow anaerobically in rather Na^+-rich environments. It is also intriguing that in some species such as *Thermotoga maritima*, Gln32 is replaced by Glu. It seems plausible, at least statistically speaking,[20] that this arrangement would also be well suited for Na^+ coordination and hence that the ATP synthase of some of these species is driven by the *smf* rather than the *pmf*. Conclusive biochemical data for these cases are still missing.

Finally, it is worth noting that mutants of Gly25 and Thr67 (Fig. 3b) to isoleucine and cysteine, respectively, have been shown to abolish ATP synthesis by purified enzymes reconstituted into proteoliposomes.[37] This underlines their functional and physiological importance in Na^+-dependent ATP synthases. The results in that study were interpreted as indicative of a hypothetical interaction between Thr67 and a conserved key arginine residue on the a-subunit interface. In the light of this study, however, it is also plausible that these mutants display a diminished ion-binding capacity or altered selectivity properties. Such an effect has indeed been observed, for example, in mutagenized rings of the proton-coupled *Escherichia coli* ATP synthase.[38] In this case, residues 60–63 were changed from Val-Asp-Ala-Ile to Ala-Asp-Ser-Thr, corresponding to residues 64–67 in *I. tartaricus*. Although this mutant enzyme could not transport or bind Na^+, it was

Table 3. Computed and experimental free energies of hydration, and of cation selectivity in the c-ring of the F_1F_o-ATPase from *I. tartaricus*

$\Delta G_{hydration}$ (C^+)	Na^+	H_2O
Computed	−89.3	−6.5
Experimental	−90.7[a]	−6.3[b]
ΔG_{bulk} ($C_1^+ \rightarrow C_2^+$)	$Na^+ \rightarrow K^+$	$Na^+ \rightarrow Li^+$
Computed	18.2±0.1	−25.4±0.1
Experimental	17.2[c]	25.2[c]
$\Delta\Delta G_{sel}$ ($C_1^+ \rightarrow C_2^+$)	$Na^+ \rightarrow K^+$	$Na^+ \rightarrow Li^+$
Computed w/ H_2O	6.0±0.3	1.3±0.2
Computed w/o H_2O	2.5±0.6	0.7±0.2
Experimental	>3.7[d]	~1.4[d]

All data are expressed in kilocalories per mole. Selectivity calculations were repeated for three binding sites in the ring, in the forward and backward directions. The values reported are averages, with the corresponding standard deviations.

[a] From Kelly *et al.*,[45] after correcting for the potential of the water–air interface, which was estimated to be 12.45 kcal/mol.[46]

[b] From Camaioni and Schwerdtfeger.[47]

[c] From Kelly *et al.*[45]

[d] From Kluge and Dimroth[7] and Meier and Dimroth,[15] using $\Delta\Delta G_{sel} = -k_B T \log K_d/K_i$.

certainly inhibited by Li^+. At any rate, the side chain at position 67 and the coordinating water molecule (Fig. 3b) are two key elements that need to be considered from now on in order to elucidate the mechanism of Na^+ translocation through the F_o complex and to understand how this process powers ATP synthesis at the molecular level.

Materials and Methods

Crystallographic analysis

The improved structure of the *I. tartaricus* c_{11}-ring originates from the same diffraction data set for which details were reported in Meier *et al.*[8] These data were re-reduced, for the present work, with the latest XDS version (January 2009).[39] Refinement was initiated using the c_{11}-ring model from PDB ID code 1yce, representing the final result of Refmac[40] refinement in 2004. Algorithmic improvements, most importantly a more stable TLS model and a more realistic solvent modeling in PHENIX.refine,[41] allowed a slightly wider resolution range (40–2.35 Å). The same set of reflections selected for the calculation of free *R*-factors was used as established for PDB ID code 1yce. In order to prevent bias in the identification of the electron density corresponding to the 44 additional water binding sites in the same asymmetric unit, we first refined without imposing any noncrystallographic symmetry. After an unambiguous identification of the additional waters, they were included in the model in the last rounds of the refinement. The R_{work} and R_{free} values of the model against the data do not rise steeply near the high-resolution cutoff, attesting to its correct choice and consistent with an I/σ_I value significantly higher than 1.

MD and free-energy calculations

All MD simulations and free-energy calculations were carried out with NAMD[42] using the CHARMM27 force field,[43] at constant temperature (298 K) and pressure

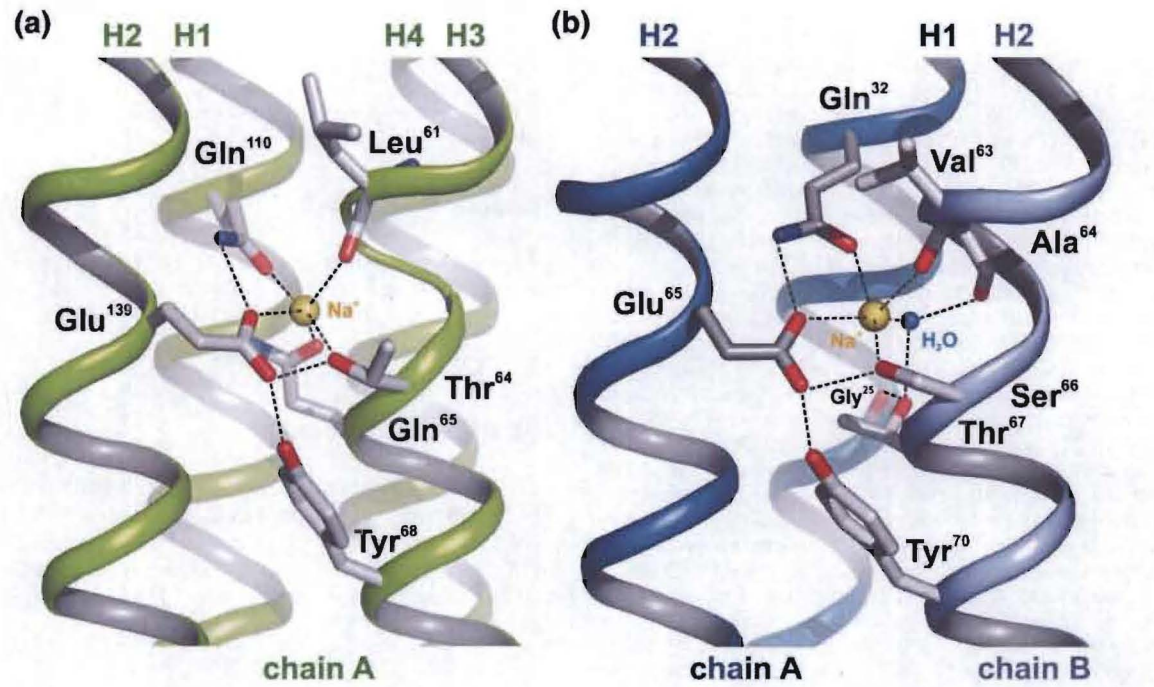

Fig. 3. Na^+ binding in the rotor rings of the V-ATPase from *E. hirae* and the F-ATP synthase from *I. tartaricus*. (a) In the K_{10}-ring from *E. hirae* (PDB ID code 2bl2),[12] Na^+ is coordinated within a single K-subunit, each of which comprises four α-helices (H1–H4; green). (b) In the c_{11}-ring from *I. tartaricus*,[8] the Na^+ binding site is located in between the inner (H2; blue) and the outer (H1; blue) helices of one c-subunit, and the outer helix (H2; purple) of the adjacent c-subunit. Dashed lines indicate ion-coordination contacts and the network of hydrogen bonds at the site.

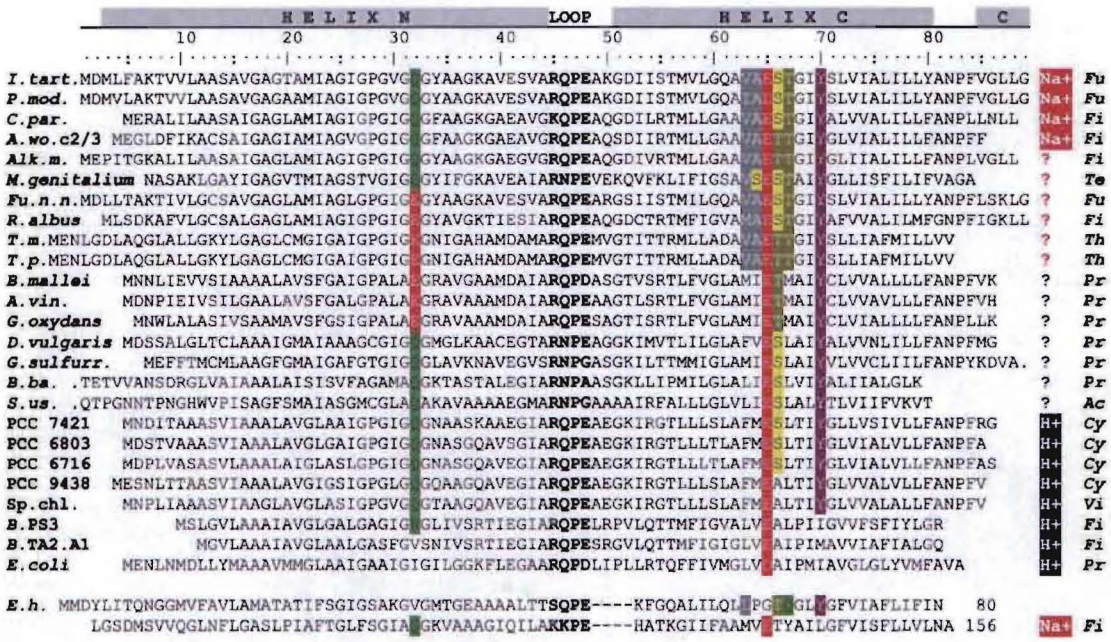

Fig. 4. Alignment of c-subunit sequences from F-ATP synthases of selected species. Individual sequences were aligned according to the cytoplasmic loop region (bold). The single c-subunits form α-helical hairpins; the location of the N-terminal and C-terminal helices is indicated in gray. The type of ion coordination (Na^+ or H^+) is indicated on the right (ion). Residues involved in Na^+ coordination and discussed in this work are indicated in colors. Species names: *I. tartaricus* (numbering), *P. modestum*, *C. paradoxum*, *A. woodii*, *Alkaliphilus metalliredigens*, *Mycoplasma genitalium*, *Fusobacterium nucleatum* subsp. *nucleatum*, *Ruminococcus albus*, *T. maritima*, *Thermotoga petrophila*, *Burkholderia mallei*, *Azotobacter vinelandii*, *Gluconobacter oxydans*, *Desulfovibrio vulgaris*, *Geobacter sulfurreducens*, *Solibacter usitatus*, *Bdellovibrio bacteriovorus*, *Gloeobacter violaceus* PCC 7421, *Synechocystis* sp. strain PCC 6803, *Synoechococcus* sp. strain PCC 6716, *Arthrospira* sp. strain PCC 9438 (*Spirulina platensis* C1), spinach choloroplast, *Bacillus* sp. strain PS3, *Bacillus* sp. strain TA2.A1, *E. coli*; V-ATPase: *E. hirae*. The abbreviated phyla (p) names are: *Fu*, Fusobacteria; *Fi*, Firmicutes; *Te*, Tenericutes; *Th*, Thermotogae; *Pr*, Proteobacteria; *Ac*, Acidobacteria; *Vi*, Viridiplantae.

(1 atm), under periodic boundary conditions. Electrostatic interactions were computed using the particle–mesh Ewald algorithm with a real-space cutoff distance at 14 Å, which was also used for van der Waals interactions. Simulations of bulk systems included 1000 molecules in a cubic box of ~31 Å on each side, pressure-coupled isotropically. In the protein–lipid system, the pressure was applied only along the membrane normal, while the surface area of the membrane (POPC) was kept constant (~69 $Å^2$ per lipid). The simulation of the complete c-ring in the POPC membrane was prepared using the methodology described by Faraldo-Gómez *et al.*, now implemented into NAMD.[44] This model comprises 237 POPC lipids and approximately 18,000 water molecules in addition to the protein (i.e., a total of ~100,000 atoms) (Fig. S2). To equilibrate this molecular model, we carried out conventional MD simulations with gradually weaker constraints on the protein structure for up to 10 ns. Subsequent unrestrained simulations of 15 ns duration were used for analysis and as starting point for free-energy calculations. The free-energy perturbation method was used in the calculations of water binding affinity and ion selectivity. As is common, we followed a stepwise protocol, through a coupling parameter λ, in the forward and backward directions. Between 25 and 30 intermediate λ steps were used in each case, with sampling times ranging between 200 ps and 1 ns per step. A pseudo-soft-core potential was used in the calculations of water binding affinity, with a cutoff at 1.3 Å. Parameters for the cations considered in this study were initially derived from Noskov and Roux[18] and very slightly adjusted to better match relative hydration-free energies[45] as computed under our simulation conditions, as well as the ion selectivity measurements for the K-ring.[17] Further details are given in Supplementary Data (Fig. S3).

Accession numbers

Coordinates and structure factors have been deposited in the PDB with accession number 2wgm.

Acknowledgements

This work was supported, in part, by the Cluster of Excellence "Macromolecular Complexes" at the JW Goethe University Frankfurt (DFG project EXC 115) and the DFG (German Research Foundation). P.J.B. was supported by an EMBO fellowship (ALTF 1021-2007).

Supplementary Data

Supplementary data associated with this article can be found, in the online version, at doi:10.1016/j.jmb.2009.05.082

References

1. Abrahams, J. P., Leslie, A. G. W., Lutter, R. & Walker, J. E. (1994). Structure at 2.8 Å resolution of F_1-ATPase from bovine heart mitochondria. *Nature*, **370**, 621–628.
2. Boyer, P. D. (1993). The binding change mechanism for ATP synthase—some probabilities and possibilities. *Biochim. Biophys. Acta*, **1140**, 215–250.
3. Capaldi, R. A. & Aggeler, R. (2002). Mechanism of the F_1F_0-type ATP synthase, a biological rotary motor. *Trends Biochem. Sci.* **27**, 154–160.
4. Yoshida, M., Muneyuki, E. & Hisabori, T. (2001). ATP synthase—a marvellous rotary engine of the cell. *Nat. Rev. Mol. Cell Biol.* **2**, 669–677.
5. Nakamoto, R. K., Baylis Scanlon, J. A. & Al-Shawi, M.K. (2008). The rotary mechanism of the ATP synthase. *Arch. Biochem. Biophys.* **476**, 43–50.
6. Meier, T., Matthey, U., von Ballmoos, C., Vonck, J., Krug von Nidda, T., Kühlbrandt, W. & Dimroth, P. (2003). Evidence for structural integrity in the undecameric c-rings isolated from sodium ATP synthases. *J. Mol. Biol.* **325**, 389–397.
7. Kluge, C. & Dimroth, P. (1993). Specific protection by Na^+ or Li^+ of the F_1F_0-ATPase of *Propionigenium modestum* from the reaction with dicyclohexylcarbodiimide. *J. Biol. Chem.* **268**, 14557–14560.
8. Meier, T., Polzer, P., Diederichs, K., Welte, W. & Dimroth, P. (2005). Structure of the rotor ring of F-type Na^+-ATPase from *Ilyobacter tartaricus*. *Science*, **308**, 659–662.
9. Valiyaveetil, F. I. & Fillingame, R. H. (1997). On the role of Arg-210 and Glu-219 of subunit a in proton translocation by the *Escherichia coli* F_0F_1-ATP synthase. *J. Biol. Chem.* **272**, 32635–32641.
10. Wehrle, F., Kaim, G. & Dimroth, P. (2002). Molecular mechanism of the ATP synthase's F_o motor probed by mutational analyses of subunit a. *J. Mol. Biol.* **322**, 369–381.
11. Dimroth, P., von Ballmoos, C. & Meier, T. (2006). Catalytic and mechanical cycles in F-ATP synthases. *EMBO Rep.* **7**, 276–282.
12. Murata, T., Yamato, I., Kakinuma, Y., Leslie, A. G. & Walker, J. E. (2005). Structure of the rotor of the V-type Na^+-ATPase from *Enterococcus hirae*. *Science*, **308**, 654–659.
13. Neumann, S., Matthey, U., Kaim, G. & Dimroth, P. (1998). Purification and properties of the F_1F_o ATPase of *Ilyobacter tartaricus*, a sodium ion pump. *J. Bacteriol.* **180**, 3312–3316.
14. Murata, T., Takase, K., Yamato, I., Igarashi, K. & Kakinuma, Y. (1997). Purification and reconstitution of Na^+-translocating vacuolar ATPase from *Enterococcus hirae*. *J. Biol. Chem.* **272**, 24885–24890.
15. Meier, T. & Dimroth, P. (2002). Intersubunit bridging by Na^+ ions as a rationale for the unusual stability of the c-rings of Na^+-translocating F_1F_0 ATP synthases. *EMBO Rep.* **3**, 1094–1098.
16. Murata, T., Igarashi, K., Kakinuma, Y. & Yamato, I. (2000). Na^+ binding of V-type Na^+-ATPase in *Enterococcus hirae*. *J. Biol. Chem.* **275**, 13415–13419.
17. Murata, T., Yamato, I., Kakinuma, Y., Shirouzu, M., Walker, J. E., Yokoyama, S. & Iwata, S. (2008). Ion binding and selectivity of the rotor ring of the Na^+-transporting V-ATPase. *Proc. Natl Acad. Sci. USA*, **105**, 8607–8612.
18. Noskov, S. Y. & Roux, B. (2008). Control of ion selectivity in LeuT: two Na^+ binding sites with two different mechanisms. *J. Mol. Biol.* **377**, 804–918.
19. Nayal, M. & Di Cera, E. (1996). Valence screening of water in protein crystals reveals potential Na^+ binding sites. *J. Mol. Biol.* **256**, 228–234.
20. Harding, M. M. (2004). The architecture of metal coordination groups in proteins. *Acta Crystallogr. Sect. D*, **60**, 849–859.
21. Roux, B., Nina, M., Pomes, R. & Smith, J. C. (1996). Thermodynamic stability of water molecules in the bacteriorhodopsin proton channel: a molecular dynamics free energy perturbation study. *Biophys. J.* **71**, 670–681.
22. Gilson, M. K., Given, J. A., Bush, B. L. & McCammon, J. A. (1997). The statistical-thermodynamic basis for computation of binding affinities: a critical review. *Biophys. J.* **72**, 1047–1069.
23. Wang, J., Deng, Y. & Roux, B. (2006). Absolute binding free energy calculations using molecular dynamics simulations with restraining potentials. *Biophys. J.* **91**, 2798–2814.
24. Ninni, L., Camargo, M. S. & Meirelles, A. J. A. (1999). Water activity in poly(ethylene glycol) aqueous solutions. *Thermochim. Acta*, **328**, 169–176.
25. Beyer, R. & Steiger, M. (2002). Vapor pressure measurements and thermodynamic properties of aqueous solutions of sodium acetate. *J. Chem. Thermodyn.* **34**, 1057–1071.
26. Noskov, S. Y., Bernèche, S. & Roux, B. (2004). Control of ion selectivity in potassium channels by electrostatic and dynamic properties of carbonyl ligands. *Nature*, **431**, 830–834.
27. Noskov, S. Y. & Roux, B. (2007). Importance of hydration and dynamics on the selectivity of the KcsA and NaK channels. *J. Gen. Physiol.* **129**, 135–143.
28. Mulkidjanian, A. Y., Dibrov, P. & Galperin, M. Y. (2008). The past and present of sodium energetics: may the sodium-motive force be with you. *Biochim. Biophys. Acta*, **1777**, 985–992.
29. Laubinger, W. & Dimroth, P. (1987). Characterization of the Na^+-stimulated ATPase of *Propionigenium modestum* as an enzyme of the F_1F_o type. *Eur. J. Biochem.* **168**, 475–482.
30. Reidlinger, J. & Müller, V. (1994). Purification of ATP synthase from *Acetobacterium woodii* and identification as a Na^+-translocating F_1F_o-type enzyme. *Eur. J. Biochem.* **223**, 275–283.
31. Ferguson, S. A., Keis, S. & Cook, G. M. (2006). Biochemical and molecular characterization of a Na^+-translocating F_1F_o-ATPase from the thermoalkaliphilic bacterium *Clostridium paradoxum*. *J. Bacteriol.* **188**, 5045–5054.
32. Mulkidjanian, A. Y., Galperin, M. Y., Makarova, K. S., Wolf, Y. I. & Koonin, E. V. (2008). Evolutionary primacy of sodium bioenergetics. *Biol. Direct*, **3**, 13.
33. Mulkidjanian, A. Y., Galperin, M. Y. & Koonin, E. V. (2009). Co-evolution of primordial membranes and membrane proteins. *Trends Biochem. Sci.* **34**, 206–215.
34. Kaim, G., Wehrle, F., Gerike, U. & Dimroth, P. (1997). Molecular basis for the coupling ion selectivity of F_1F_0 ATP synthases: probing the liganding groups for Na^+ and Li^+ in the c subunit of the ATP synthase from *Propionigenium modestum*. *Biochemistry*, **36**, 9185–9194.
35. Feng, Y. & McCarty, R. E. (1990). Chromatographic purification of the chloroplast ATP synthase (CF_0–CF_1) and the role of CF_0 subunit IV in proton conduction. *J. Biol. Chem.* **265**, 12474–12480.
36. Van Walraven, H. S., Strotmann, H., Schwarz, O. & Rumberg, B. (1996). The H^+/ATP coupling ratio of the ATP synthase from thiol-modulated chloroplasts and

two cyanobacterial strains is four. *FEBS Lett.* **379**, 309–313.
37. Vorburger, T., Ebneter, J. Z., Wiedenmann, A., Morger, D., Weber, G., Diederichs, K. *et al.* (2008). Arginine-induced conformational change in the c-ring/a-subunit interface of ATP synthase. *FEBS J.* **275**, 2137–2150.
38. Zhang, Y. & Fillingame, R. H. (1995). Changing the ion binding specificity of the *Escherichia coli* H^+-transporting ATP synthase by directed mutagenesis of subunit c. *J. Biol. Chem.* **270**, 87–93.
39. Kabsch, W. (1993). Automatic processing of rotation diffraction data from crystals of initially unknown symmetry and cell constants. *J. Appl. Crystallogr.* **26**, 795–800.
40. Collaborative Computational Project Nr. 4 (1994). The CCP4 suite: programs for protein crystallography. *Acta Crystallogr. Sect. D*, **50**, 760–763.
41. Adams, P. D., Grosse-Kunstleve, R. W., Hung, L. W., Ioerger, T. R., McCoy, A. J., Moriarty, N. W. *et al.* (2002). PHENIX: building new software for automated crystallographic structure determination. *Acta Crystallogr. Sect. D*, **58**, 1948–1954.
42. Phillips, J. C., Braun, R., Wang, W., Gumbart, J., Tajkhorshid, E., Villa, E. *et al.* (2005). Scalable molecular dynamics with NAMD. *J. Comput. Chem.* **26**, 1781–1802.
43. MacKerell, A. D., Bashford, D., Bellott, M., Dunbrack, R. L., Evanseck, J. D., Field, M. J. *et al.* (1998). All-atom empirical potential for molecular modeling and dynamics studies of proteins. *J. Phys. Chem. B*, **102**, 3586–3616.
44. Faraldo-Gómez, J. D., Smith, G. R. & Sansom, M. S. (2002). Setting up and optimization of membrane protein simulations. *Eur. Biophys. J.* **31**, 217–227.
45. Kelly, C. P., Cramer, C. J. & Truhlar, D. G. (2006). Aqueous solvation free energies of ions and ion–water clusters based on an accurate value for the absolute aqueous solvation free energy of the proton. *J. Phys. Chem. B*, **110**, 16066–16081.
46. Lamoureux, G. & Roux, B. (2006). Absolute hydration free energy scale for alkali and halide ions established from simulations with a polarizable force field. *J. Phys. Chem. B*, **110**, 3308–3322.
47. Camaioni, D. M. & Schwerdtfeger, C. A. (2005). Comment on Accurate experimental values for the free energies of hydration of H^+, OH^-, and H_3O^+. *J. Phys. Chem. A*, **109**, 10795–10797.